THE JOURNAL OF PHYSICAL CHEMISTRY LETTERS
A JOURNAL OF THE AMERICAN CHEMICAL SOCIETY

pubs.acs.org/JPCL Letter

Direct Observation of the C + S_2 Channel in CS_2 Photodissociation

Zhenxing Li, Min Zhao, Ting Xie, Zijie Luo, Yao Chang, Gongkui Cheng, Jiayue Yang, Zhichao Chen, Weiqing Zhang, Guorong Wu, Xingan Wang,* Kaijun Yuan,* and Xueming Yang

Cite This: *J. Phys. Chem. Lett.* 2021, 12, 844−849 Read Online

ABSTRACT: Carbon disulfide (CS_2) is a typical triatomic molecule. Its photodissociation process has generally been assumed to proceed to CS and S primary products via single bond fission. However, recent theoretical calculations suggested that an exit channel to produce C + S_2 should also be energetically accessible. Here, we report the direct experimental evidence for the C + S_2 channel in CS_2 photodissociation by using the velocity map ion imaging technique with two-photon UV and one-photon vacuum UV (VUV) excitations. The detection of the C (^{3}P) products illustrates that the ground state and the electronically excited states of S_2 coproducts are formed within highly excited vibrational states. The very weak anisotropic distributions indicate relatively slow dissociation processes. The possible dissociation mechanism involves molecular isomerization of CS_2 to *linear*-CSS from the excited $^1B_2$ ($2^1\Sigma^+$) state via vibronic coupling with the $^1\Pi$ state followed by an avoided crossing with the ground state surface. Our results imply that the S_2 molecules observed in comets might be primarily formed in CS_2 photodissociation.

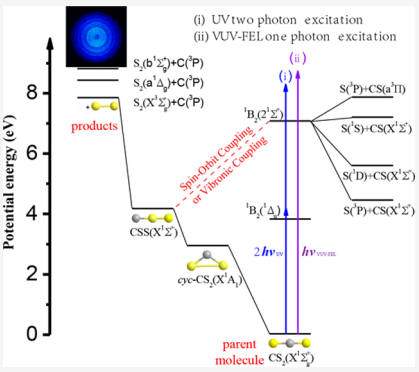

Photodissociation dynamics of triatomic molecules has been a field of intensive research, as these systems are amenable to detailed experimental and theoretical studies that could significantly deepen our understanding of photochemistry. Over the past few decades, the textbook mechanism for a triatomic molecule ABC mainly involves single bond fission to produce A + BC or AB + C.[1] However, recent investigations on CO_2 (*linear*−OCO)[2] and OCS[3] photolysis have revealed the central-atom elimination processes, i.e., C + O_2 and C + SO channels, which could take place via either a conventional nonadiabatic dissociation pathway or a roaming pathway. Intriguing questions would be does this central-atom elimination channel exist in the photodissociation processes of other triatomic molecules and does this process involve another detailed microscopic mechanism?

As a typical triatomic molecule, CS_2 possesses 16 valence electrons with a linear centrosymmetric structure (SCS). Because of its importance in astrophysical media, the earth's atmosphere, biological media, and organic chemistry, the photodissociation behavior of its low-lying singlet and triplet electronic states have been extensively studied theoretically[4−8] and experimentally.[9−13] The absorption spectrum of CS_2 shows many absorption bands between 100 and 400 nm,[14] and the photochemistry of CS_2 in this region has been a subject of active interest for more than half a century, due to its strong dependence on the wavelength of photolysis. Absorption of one photon around 193 nm leads to the production of singlet CS ($X^1\Sigma^+$) fragments and sulfur atoms in the triplet or singlet state (^{3}P or ^{1}D).[15,16] The branching ratio for the S (^{3}P) and S (^{1}D) channels reported from these studies varies remarkably, from 0.25 to 6.[17−19] For photolysis wavelengths toward the vacuum ultraviolet (VUV) region, the production of triplet CS ($a^3\Pi$) becomes more important, and between 140 and 125 nm, the CS fragments are almost completely produced in the triplet state.[20] The possible dissociation channels concerning CS and S fragments are summarized in Figure 1.

Recently, the CS and S_2 radicals have been both observed by radio and ultraviolet (UV) spectroscopies in several comets.[21] Theoretical calculations suggested that the UV irradiation of CS_2 may induce photochemical processes responsible for the production of CS and S_2 radicals in comets.[22] On the other hand, Jimenz-Escobar and co-workers proposed H_2S_2, formed after the X-ray radiation of H_2S ices, as the parent for S_2 production in comets.[23] In fact, whether S_2 is "a parent or a daughter" is still unknown; regardless, S_2 is very short-lived.

Although one speculates that the central-atom elimination channel may widely exist in the photodissociation processes of triatomic molecules, such a process has not been observed in triatomic molecule systems other than CO_2 and OCS yet. There have been several reports of CS_2 photochemistry that have tried to illustrate the formation mechanism of S_2 fragments. In one study, de Sorgo et al.[24] observed transient

Received: November 13, 2020
Accepted: January 7, 2021
Published: January 11, 2021

https://dx.doi.org/10.1021/acs.jpclett.0c03386
J. Phys. Chem. Lett. 2021, 12, 844−849

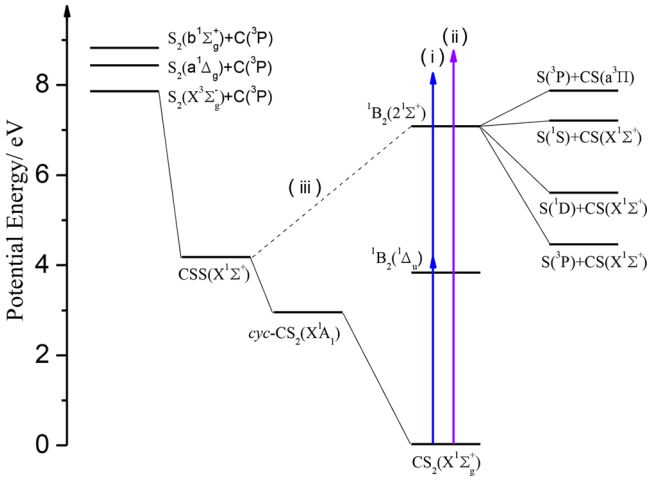

Figure 1. Plausible mechanisms of the photodissociation of CS_2. (i) Two-photon excitation with the wavelengths between 300 and 320 nm. (ii) One-photon excitation by using the VUV FEL laser in the wavelength region of 128−144 nm. (iii) The wavepacket explores the flat potential energy surface of $^1B_2(2^1\Sigma^+)$, and spin−orbit or vibronic couplings may occur, leading to S + CS or conversion to linear CSS.

absorption spectra of S_2 ($v = 0$), but no S atoms were observed by that method. They concluded that S_2 must be formed by the reaction $CS_2^* + CS_2 \rightarrow 2CS + S_2$. In other studies, Makarov and Bazhin,[25] and more recently Makarov,[26] suggested the formation of S_2 would probably occur in small clusters of CS_2 and provided a model for a new style of cluster photochemistry: $(CS_2)_2^* \rightarrow (CS)_2 + S_2$. More recently, Sapers et al.[27] proposed that CS_2 excited in the region of 300 nm absorbs a second photon with a high cross section to a high-lying state at around 8.05 eV, where the molecule predissociates to CS + S; the S atoms thus then react with CS_2 to give S_2 and CS. To date, however, the direct evidence of the S_2 product from CS_2 photolysis has not yet been observed.

Recent theoretical calculation[28] by Trabelsi et al. suggested that an exit channel to produce C + S_2 from CS_2 photolysis with sufficient photon energy is possible. The computation showed that for bent structures, the initially excited $^1B_2$ ($2^1\Sigma^+$) state of CS_2 is crossed by the bent component of the $^1\Pi$ state; the CSS isomer can be formed after vibronic coupling with $^1\Pi$ by an avoided crossing with the ground electronic state. As shown in Figure 5b in ref 28, the formation of the cyc-CS_2 from the linear CSS takes place on the flat potential energy surface of the ground state of the linear CSS. The CSS molecule has enough internal energy to convert to *cyc*-CS_2 or via fragmentation, producing C (^3P) + S_2 ($X^3\Sigma_g^-$). Despite these theoretical results, to our knowledge, there has been no experimental verification of the C + S_2 channel in CS_2 photodissociation. Here, we report the study of this interesting C + S_2 channel in CS_2 photodissociation by using two-photon and one-photon excitations. Direct experimental evidence of C (^3P) + S_2 ($X^3\Sigma_g^-/a^1\Delta_g/b^1\Sigma_g^+$) products was observed using the velocity map ion imaging (VMI) measurements of C (^3P) atoms. The photoconversion of CS_2 to *cyc*-CS_2 and *linear*-CSS is believed to play an important role in this dissociation process.

The apparatus for the VMI experiments has been described previously.[29−32] A pulsed supersonic beam was generated by expanding a mixture of 0.3% CS_2 and He into the source chamber where it was skimmed before entering and propagating along the center axis of the ion optics assembly mounted in the same differentially pumped reaction chamber. The molecular beam was intersected at 90° angles by the photolysis and probe laser beams between the second and the third plates of the ion optics assembly. The photolysis photons were provided by an Nd:YAG laser pumped dye laser (for two-photon excitation between 300 and 320 nm) and the vacuum ultraviolet free electron laser[33,34] (the VUV FEL, for one-photon excitation between 128 and 144 nm). The C (^3P) photoproducts were probed by 1 + 1′ (VUV + visible) excitation with the λ_{VUV} = 127.99 nm (resonant excitation of C ($^3P_1$)).[35] The VUV detection laser light was generated by the four-wave difference frequency mixing the frequency doubled output from one dye laser (at λ = 212.557 nm) and the fundamental output of a second dye laser (at λ = 626.57 nm) in a Kr gas cell. The visible laser beam (at λ = 700 nm) generated by a third dye laser was used as the 1′ light. The C^+ ions were then accelerated through the remaining ion optics and a 740 mm long field-free region before impacting a 70 mm diameter microchannel plate (MCP) detector coupled with a phosphor screen (P43). A charge-coupled device (CCD) camera was used to record the transient images on the phosphor screen, using a 15 ns gate pulse voltage in order to acquire time-sliced images.

As mentioned above, we first employed two-photon excitation of CS_2 in the wavelength region of 300−320 nm and VUV + visible light beams to ionize the C atom products. Figure 2 presents the ion images of C ($^3P_1$) products at two-photon photolysis wavelengths of 300.0, 303.8, 307.3, 312.9, and 320.0 nm. The double headed red arrows in the figures stand for the polarization direction of photolysis lasers. The well-resolved concentric ring structures were observed in the ion images, which correspond to individual vibrational states of S_2 coproducts. It is noted that these structures cannot arise from the other C elimination process, like the C + S + S channel, because of the insufficient photolysis photon energy. To avoid the C fragment from the secondary dissociation (the primary CS fragment may further dissociate by absorbing one UV or VUV photon), an off-axis biconvex LiF lens was used to disperse the 212.557 nm light from the direction of 127.99 nm beam, and the 127.99 nm light remains defocused.[35]

In this CS_2 photodissociation experiment, the photo-excitation energy ($h\nu$) is distributed between the C (^3P_J) and S_2 ($X^3\Sigma_g^-$) product kinetic energy (E_K) and internal energy (E_{int}), where E_{int}[C (^3P_J)] is due to excitation of the spin−orbit state; and the correlated S_2 ($X^3\Sigma_g^-$) photoproducts can be both rotationally and vibrationally excited. The VMI images can be used to determine the recoil velocity distribution of the C (^3P_J) photofragments from the radii of the resolved ring structures. The velocities are converted to a total kinetic energy release (TKER) spectrum of the C (^3P_J) + S_2 ($X^3\Sigma_g^-$) channel by using eq 1 based on the conservation of linear momentum and energy

$$h\nu = D_0 + E_{int}[C\ (^3P_J)] + E_{int}[S_2\ (X^3\Sigma_g^-)] + E_K[C\ (^3P_J) + S_2\ (X^3\Sigma_g^-)] \quad (1)$$

Here, D_0 is the thermochemical threshold for the formation of the C (^3P_J) + S_2 ($X^3\Sigma_g^-$) products from CS_2 dissociation, which was determined to be 7.86 eV (157.7 nm) by Fournier et al.[36] However, our experiments have recorded the image of C ($^3P_0$) at the longest wavelength of ∼333 nm (Figure S1), suggesting the thermochemical threshold of C ($^3P_0$) + S_2 ($X^3\Sigma_g^-$) channel should be lower than 7.45 eV (166.5 nm).

https://dx.doi.org/10.1021/acs.jpclett.0c03386
J. Phys. Chem. Lett. 2021, 12, 844−849

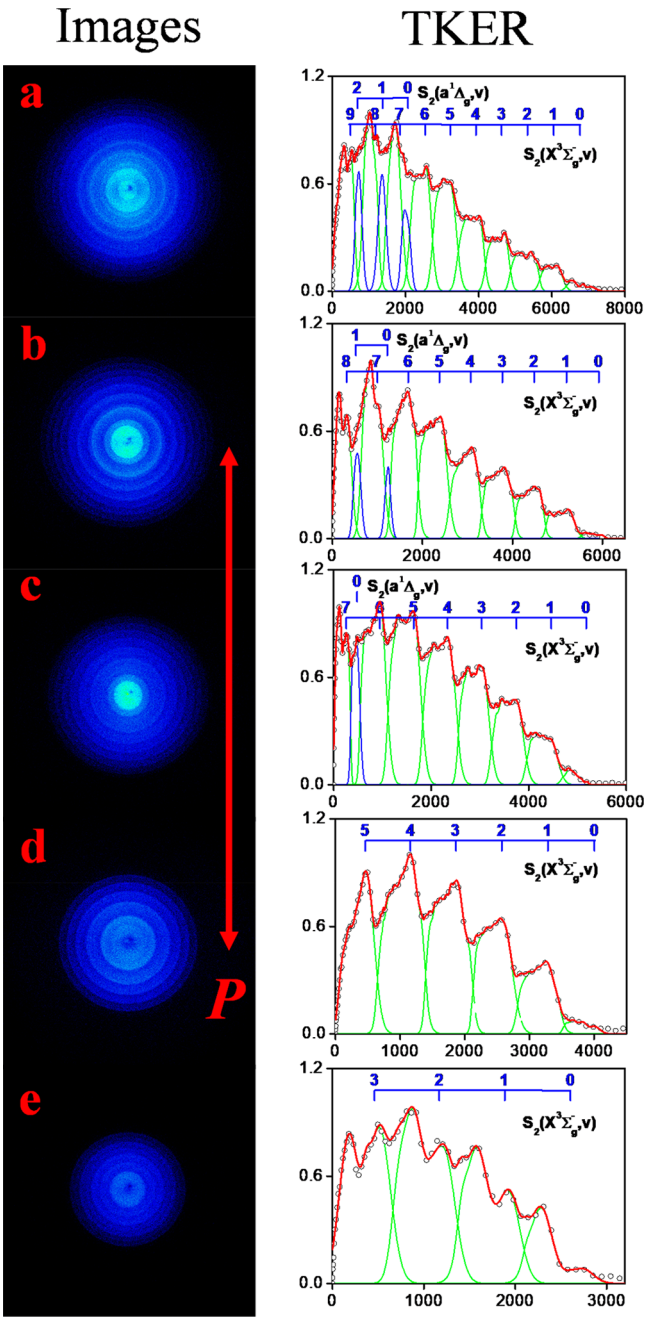

Figure 2. Ion images and translational energy distributions (arb. units) of C ($^3P_1$) products from two-photon dissociation of CS_2 at wavelengths of (a) 300.0, (b) 303.8, (c) 307.3, (d) 312.9, and (e) 320.0 nm. The rings shown in the images correspond to the vibrational state of the S_2 ($X^3\Sigma_g^-$) and S_2 ($a^1\Delta_g$) coproducts.

Figure 2 displays the TKER distributions of the C ($^3P_1$) channel by integrating over all product angles. The internal energy distributions of S_2 ($X^3\Sigma_g^-$) coproducts can be obtained from the TKER spectra by using the law of energy conservation. The energy combs representing the vibrational quantum numbers of S_2 ($X^3\Sigma_g^-$) products are labeled in Figure 2. Since the first electronically excited state of S_2 ($a^1\Delta_g$) is estimated to be ~4700 cm^{-1} higher than the ground state,[37] the vibrational progressions of S_2 ($a^1\Delta_g$) products are also displayed in Figure 2. We have also acquired C (^3P_J) images for the three spin−orbit states (J = 0, 1, and 2) (Figure S2), which show almost the same distributions. This implies that the spin−orbit interaction plays a minor role in this dissociation channel.

In order to abstract more information, a qualitative simulation of the energy distribution was carried out. The results of the simulation reveal that the rotational distributions of S_2 ($X^3\Sigma_g^-$) are narrow and appear to peak at a low J at all of the investigated wavelengths. This cold product rotational temperature indicates that the bending motion of the CS_2 molecule is not extensively excited along the dissociation coordinate, and the dissociating CS_2 molecule probably possesses a near linear geometry. Figure 3 shows the relative

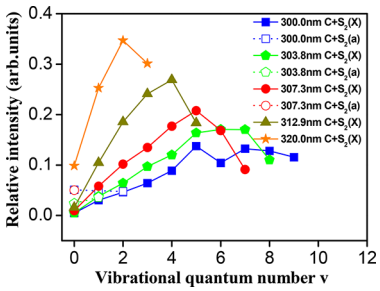

Figure 3. Relative population of different vibrational states of the S_2 ($X^3\Sigma_g^-$) and S_2 ($a^1\Delta_g$) coproducts from the C ($^3P_1$) detection at five photolysis wavelengths.

vibrational state populations of S_2 products. The S_2 ($X^3\Sigma_g^-$) products are obviously highly vibrationally excited, with the largest population at v = 2, 4, 5, 7, and 5 for the photolysis wavelengths 300.0, 303.8, 307.3, 312.9, and 320.0 nm, respectively. It is noted that the S_2 ($X^3\Sigma_g^-$) products show quite similar distributions at all five photolysis wavelengths, suggesting a similar dissociation mechanism in this wavelength region. The population of the S_2 ($a^1\Delta_g$) products is small and a little arbitrary, since there is no clear sign to separate the TKER spectra of S_2 ($X^3\Sigma_g^-$) and S_2 ($a^1\Delta_g$) products.

The product spatial angular distribution was also obtained by the following equation

$$f(\theta) = \sigma\{1 + \beta_2 P_2(\cos\theta) + \beta_4 P_4(\cos\theta)\} \quad (2)$$

where σ is the product translational energy distribution, β_2 and β_4 are anisotropy parameters that depend on the photodissociation rates for the formation of specific photofragments and the geometry of the excited molecule, P_2 and P_4 are the second- and fourth-order Legendre polynomials, and θ is the scattering angle. The overall angular parameters were determined by fitting the angular distributions in Figure 2. Table 1 lists the overall anisotropy parameters of C ($^3P_1$) products at the five photolysis wavelengths. The averaged β_2 values over the product translational energy distribution are ~0.2 for C ($^3P_1$) products at the five wavelengths, while the

Table 1. Anisotropy Parameter Values Derived from Simulations of Differential Cross Sections for C ($^3P_1$) Photoproducts by Using Eq 2

wavelengths/nm	β_2	β_4
300.0	0.23	−0.01
303.8	0.23	−0.02
307.3	0.20	−0.02
312.9	0.18	−0.04
320.0	0.12	−0.02

https://dx.doi.org/10.1021/acs.jpclett.0c03386
J. Phys. Chem. Lett. 2021, 12, 844−849

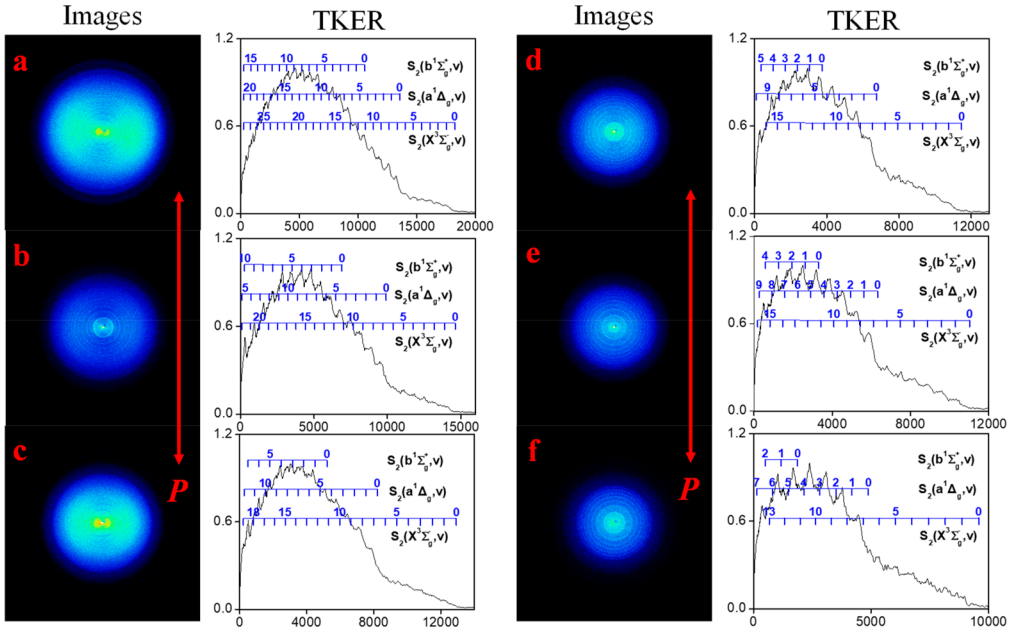

Figure 4. Ion images and translational energy distributions (arb. units) of C ($^3P_1$) products from one-photon dissociation of CS_2 by using the VUV FEL laser at wavelengths of (a) 127.9, (b) 134.2, (c) 137.3, (d) 140.1, (e) 141.0, and (f) 143.9 nm. The rings shown in the images correspond to the vibrational state of the S_2 ($X^3\Sigma_g^-$), S_2 ($a^1\Delta_g$), and S_2 ($b^1\Sigma_g^+$) coproducts.

averaged β_4 values are close to zero. According to previous studies, the absorption band in the region of 290−330 nm of CS_2 has been assigned as a V-band, corresponding to the $^1B_2$ ($^1\Delta_u$) ← $X^1\Sigma_g^+$ transition.[38,39] This $^1B_2$ state has a quite long lifetime; thus, the angular distribution is determined solely by the second transition from the intermediate $^1B_2$ state to the final state, and the coherence between the first and the second photons would not be important.[40] From our previous paper, two-photon excitation of CS_2 around 300 nm should be via the sequential transition $^1B_2$ ($2^1\Sigma^+$) ←$^1B_2$ ($^1\Delta_u$) ←$X^1\Sigma^+$, as displayed in Figure 1. The parallel transition in the second step has led to a β_2 value of around 0.6−0.7 for the CS ($X^1\Sigma_g^+$) products between 300 and 320 nm.[35] In contrast, the β_2 value is much smaller (∼0.2) for the S_2 ($X^3\Sigma_g^-$) coproducts, suggesting a much slower dissociation process for the latter. This is rational, because the molecule needs to undergo the isomerization from the CS_2 to *linear*-CSS and then dissociates.

To explore more about the dissociation mechanism, we have also performed one-photon excitation of CS_2 by using the VUV FEL laser in the wavelength region of 128−144 nm. Figure 4 displays the C ($^3P_1$) ion images following CS_2 photodissociation at 127.9, 134.2, 137.3, 140.1, 141.0, and 143.9 nm, respectively. Each image was obtained by accumulating the C^+ signals over 30 000 laser shots with background subtraction. The red vertical arrow indicates the polarization direction of the VUV FEL laser. The TKER distributions derived from these images are also shown in Figure 4. The TKER spectra contains multiple dissociation channels, namely, C ($^3P_1$) + S_2 ($X^3\Sigma_g^-$), C ($^3P_1$) + S_2 ($a^1\Delta_g$), and C ($^3P_1$) + S_2 ($b^1\Sigma_g^+$). The energy resolution of the TKER spectra is not high enough to clearly separate the dissociation pathways to the different electronic states of S_2. The may be due to multiple product channels or the relatively higher rotational excitation of the S_2 products. Nevertheless, from the sharp steps at the high energy onset of the S_2 ($a^1\Delta_g$) products, it is rational to point out that the production of C ($^3P_1$) + S_2 ($a^1\Delta_g$) competes with that of C ($^3P_1$) + S_2 ($X^3\Sigma_g^-$). The partially resolved structures in the TKER spectra at these wavelengths illustrate that both channels are highly vibrationally excited. No such features have been found for the higher channels C ($^3P_1$) + S_2 ($b^1\Sigma_g^+$). There are several pronounced in the TKER that are in very good agreement with the energy level of the S_2 (b) state. Therefore, the S_2 (b) channel should play a role in the dissociation. However, since the S_2 (b) state has some energy overlap with other states, and the TKER spectra drops dramatically at very low kinetic energy, the intensities of S_2 ($b^1\Sigma_g^+$) products should be very small.

The angular distributions have been extracted from the images by integrating the intensity over the corresponding radical range. The C ($^3P_1$) ion images reveal slightly perpendicular distributions with average parameters around −0.1 to −0.3 at the six photolysis wavelengths. The relatively small values show very weak anisotropic distribution, indicating that this dissociation process should be quite slow, which is similar to that observed in the two-photon UV excitation experiments. Theoretical calculations[28] pointed out that the $^1B_2$ ($2^1\Sigma^+$) state of CS_2 should play a major role in the isomerization and photodissociation processes occurring at high energies. Absorption of one photon with $h\nu \geq 7.08$ eV should efficiently populate the $^1B_2$ ($2^1\Sigma^+$) state, since the transition dipole moment of the SCS $^1B_2$ ($2^1\Sigma^+$) ← $X^1\Sigma^+$ is relatively large. In this work, CS_2 molecules are excited either directly to $^1B_2$ ($2^1\Sigma^+$) state or to even higher electronic states following internal conversion to the $^1B_2$ ($2^1\Sigma^+$) state by absorbing two photons (300−320 nm) or one photon (128−144 nm). As shown in Figure 3 and Figure 5a in ref 28, the potential of $^1B_2$ ($2^1\Sigma^+$) state is shallow and flat along the CS distance and bending angle, and a molecule on this surface will undergo large-amplitude motions, which lead to several processes in competition. For instance, the $^1B_2$ ($2^1\Sigma^+$) state is crossed by the $1^1\Pi$ state for the linear configuration (with energies of ∼7 eV). After UV absorption, the S (^1D) + CS ($X^1\Sigma_g^+$) products can be formed through vibronic coupling with $1^1\Pi$. In addition, S (^3P) + CS ($X^1\Sigma_g^+$) products can occur

https://dx.doi.org/10.1021/acs.jpclett.0c03386
J. Phys. Chem. Lett. 2021, 12, 844−849

after spin−orbit coupling with the $^3\Pi$ electronic states. For bent structures, the $^1B_2$ ($2^1\Sigma^+$) state is crossed by the bent component of the $^1A_1(1^1\Pi)$ state. The CSS isomer can be formed after vibronic coupling with $^1A_1$ ($1^1\Pi$) state followed by an avoided crossing with the ground state at 115°. Finally, CSS could dissociate to C ($^3P_1$) + S_2 ($X^3\Sigma_g^-$) through a barrier without coupling to another electronic state. While higher electronic states should be involved in the S_2 ($a^1\Delta_g/b^1\Sigma_g^+$) channels, the detailed potential energy surface information awaits further theoretical investigations. Our experiments here clearly identify that the S_2 molecule can be a daughter of CS_2 in astrophysical media. The formation of S_2 from the CS_2 by two-photon UV or one-photon VUV photolysis is followed by dissociation mechanisms proposed by theoretical calculations.[28]

In summary, we have investigated the central-atom elimination channel of C + S_2 in the CS_2 photodissociation process. In both the two-photon and one-photon excitation experiments, we have clearly observed the S_2 products in its ground state ($X^3\Sigma_g^-$) and electronically excited states ($a^1\Delta_g$, $b^1\Sigma_g^+$). The dissociation mechanism involves photoconversion from CS_2 to *linear*-CSS and then dissociates after excitation to the $^1B_2$ ($2^1\Sigma^+$) or higher electronic states. Given the similarity of OCS, CO_2, and CS_2, we believe that the central-atom elimination channel is more general than expected in the photodissociation of triatomic molecules and should be added into the textbook dissociation dynamics models.

■ ASSOCIATED CONTENT

Supporting Information

The Supporting Information is available free of charge at https://pubs.acs.org/doi/10.1021/acs.jpclett.0c03386.

Additional experimental results for two-photon dissociation (PDF)

■ AUTHOR INFORMATION

Corresponding Authors

Xingan Wang − *Hefei National Laboratory for Physical Sciences at the Microscale and Department of Chemical Physics, University of Science and Technology of China, Hefei, Anhui 230026, P. R. China;* orcid.org/0000-0002-1206-7021; Email: xawang@ustc.edu.cn

Kaijun Yuan − *State Key Laboratory of Molecular Reaction Dynamics, Dalian Institute of Chemical Physics, Chinese Academy of Sciences, Dalian 116023, China;* orcid.org/0000-0002-5108-8984; Email: kjyuan@dicp.ac.cn

Authors

Zhenxing Li − *Hefei National Laboratory for Physical Sciences at the Microscale and Department of Chemical Physics, University of Science and Technology of China, Hefei, Anhui 230026, P. R. China*

Min Zhao − *Hefei National Laboratory for Physical Sciences at the Microscale and Department of Chemical Physics, University of Science and Technology of China, Hefei, Anhui 230026, P. R. China*

Ting Xie − *Hefei National Laboratory for Physical Sciences at the Microscale and Department of Chemical Physics, University of Science and Technology of China, Hefei, Anhui 230026, P. R. China*

Zijie Luo − *State Key Laboratory of Molecular Reaction Dynamics, Dalian Institute of Chemical Physics, Chinese Academy of Sciences, Dalian 116023, China*

Yao Chang − *State Key Laboratory of Molecular Reaction Dynamics, Dalian Institute of Chemical Physics, Chinese Academy of Sciences, Dalian 116023, China*

Gongkui Cheng − *State Key Laboratory of Molecular Reaction Dynamics, Dalian Institute of Chemical Physics, Chinese Academy of Sciences, Dalian 116023, China*

Jiayue Yang − *State Key Laboratory of Molecular Reaction Dynamics, Dalian Institute of Chemical Physics, Chinese Academy of Sciences, Dalian 116023, China*

Zhichao Chen − *State Key Laboratory of Molecular Reaction Dynamics, Dalian Institute of Chemical Physics, Chinese Academy of Sciences, Dalian 116023, China*

Weiqing Zhang − *State Key Laboratory of Molecular Reaction Dynamics, Dalian Institute of Chemical Physics, Chinese Academy of Sciences, Dalian 116023, China*

Guorong Wu − *State Key Laboratory of Molecular Reaction Dynamics, Dalian Institute of Chemical Physics, Chinese Academy of Sciences, Dalian 116023, China;* orcid.org/0000-0002-0212-183X

Xueming Yang − *State Key Laboratory of Molecular Reaction Dynamics, Dalian Institute of Chemical Physics, Chinese Academy of Sciences, Dalian 116023, China; Department of Chemistry, College of Science, Southern University of Science and Technology, Shenzhen 518055, China;* orcid.org/0000-0001-6684-9187

Complete contact information is available at: https://pubs.acs.org/10.1021/acs.jpclett.0c03386

Notes

The authors declare no competing financial interest.

■ ACKNOWLEDGMENTS

The experimental work is supported by the Chemical Dynamics Research Center (Grant No. 21688102), the National Natural Science Foundation of China (NSFC Nos. 21873099, 21922306, 21590802), the Key Technology Team of the Chinese Academy of Sciences (Grant No. GJJSTD20190002), the international partnership program of Chinese Academy of Sciences (No. 121421KYSB20170012), and the Strategic Priority Research Program of the Chinese Academy of Sciences (Grant No. XDB17000000). We thank Wentao Chen for helpful discussions. We also thank the staff team of the Dalian Coherent Light Source (DCLS) for technical support.

■ REFERENCES

(1) Okabe, H. *Photochemistry of Small Molecules*; Wiley: New York, 1978.

(2) Lu, Z.; Chang, Y. C.; Yin, Q. Z.; Ng, C. Y.; Jackson, W. M. Evidence for Direct Molecular Oxygen Production in CO_2 Photodissociation. *Science* **2014**, *346* (6205), 61−64.

(3) Chen, W. T.; Zhang, L.; Yuan, D. F.; Chang, Y.; Yu, S. R.; Wang, S. W.; Wang, T.; Jiang, B.; Yuan, K. J.; Yang, X. M.; et al. Observation of the Carbon Elimination Channel in Vacuum Ultraviolet Photodissociation of OCS. *J. Phys. Chem. Lett.* **2019**, *10* (17), 4783−4787.

(4) Tseng, D. C.; Poshusta, R. D. Ab-Initio Potential Energy Curves for Low-Lying States of Carbon-Disulfide. *J. Chem. Phys.* **1994**, *100* (10), 7481−7486.

(5) Zhang, Q. G.; Vaccaro, P. H. Ab-Initio Studies of Electronically Excited Carbon-Disulfide. *J. Phys. Chem.* **1995**, *99* (6), 1799−1813.

(6) Brown, S. T.; Van Huis, T. J.; Hoffman, B. C.; Schaefer, H. F. Excited Electronic States of Carbon Disulphide. *Mol. Phys.* **1999**, *96* (4), 693−704.
(7) Wiberg, K. B.; Wang, Y.; de Oliveira, A. E.; Perera, S. A.; Vaccaro, P. H. Comparison of CIS- and EOM-CCSD-Calculated Adiabatic Excited-State Structures. Changes in Charge Density on going to Adiabatic Excited States. *J. Phys. Chem. A* **2005**, *109* (3), 466−477.
(8) Pradhan, E.; Carreon-Macedo, J. L.; Cuervo, J. E.; Schroder, M.; Brown, A. Ab Initio Potential Energy and Dipole Moment Surfaces for CS_2: Determination of Molecular Vibrational Energies. *J. Phys. Chem. A* **2013**, *117* (32), 6925−6931.
(9) Brasen, G.; Demtroder, W. Vibrational Levels and Statistical Analysis of the $X^1\Sigma^+_g$ Ground State of CS_2. *J. Chem. Phys.* **1999**, *110* (24), 11841−11849.
(10) Lo, W. J.; Wu, Y. J.; Lee, Y. P. Ultraviolet Absorption Spectrum of Cyclic S_2O in Solid Ar. *J. Phys. Chem. A* **2003**, *107* (36), 6944−6947.
(11) Sunanda, K.; Shastri, A.; Das, A. K.; Sekhar, B. R. Electronic States of Carbon Disulphide in the 5.5−11.8 eV Region by VUV Photo Absorption Spectroscopy. *J. Quant. Spectrosc. Radiat. Transfer* **2015**, *151*, 76−87.
(12) Yang, J.; Beck, J.; Uiterwaal, C. J.; Centurion, M. Imaging of Alignment and Structural Changes of Carbon Disulfide Molecules using Ultrafast Electron Diffraction. *Nat. Commun.* **2015**, *6*, 8172.
(13) Dayan, E.; Dervil, E.; Loisel, J.; Pinan-Lucarre, J.P.; Tarjus, G. Interaction-Induced Vibrational Spectra of Liquid CS_2 in Various Solvents. Concentration Effect. *Chem. Phys.* **1988**, *119* (1), 107−123.
(14) McGlynn, S. P.; Rabalais, J. W.; McDonald, J. R.; Scherr, V. M. Electronic Spectoscopy of Isoelectronic Molecules. II. Linear Triatomic Groupings Containing Sixteen Valence Electrons. *Chem. Rev.* **1971**, *71* (1), 73−108.
(15) Waller, I. M.; Hepburn, J. W. Photofragment Spectroscopy of CS_2 at 193 nm - Direct Resolution of Singlet and Triplet Channels. *J. Chem. Phys.* **1987**, *87* (6), 3261−3268.
(16) Kitsopoulos, T. N.; Gebhardt, C. R.; Rakitzis, T. P. Photodissociation Study of CS_2 at 193 nm Using Slice Imaging. *J. Chem. Phys.* **2001**, *115* (21), 9727−9732.
(17) Tzeng, W. B.; Yin, H. M.; Leung, W. Y.; Luo, J. Y.; Nourbakhsh, S.; Flesch, G. D.; Ng, C. Y. A 193 nm Laser Photofragmentation Time-of-Flight Mass-Spectrometric Study of CS_2 and CS_2 Clusters. *J. Chem. Phys.* **1988**, *88* (3), 1658−1669.
(18) McGivern, W. S.; Sorkhabi, O.; Rizvi, A. H.; Suits, A. G.; North, S. W. Photofragment Translational Spectroscopy with State-Selective "Universal Detection": The Ultraviolet Photodissociation of CS_2. *J. Chem. Phys.* **2000**, *112* (12), 5301−5307.
(19) Dornhofer, G.; Hack, W.; Langel, W. Electronic Excitation and Quenching of CS Formed in the ArF Laser Photolysis of CS_2. *J. Phys. Chem.* **1984**, *88* (14), 3060−3069.
(20) Black, G.; Sharpless, R. L.; Slanger, T. G. Production of CS ($A^3\Pi$) in Photodissociation of CS_2 below 1600 Å. *J. Chem. Phys.* **1977**, *66* (5), 2113−2117.
(21) Jackson, W. M.; Scodinu, A.; Xu, D. D.; Cochran, A. L. Using the Ultraviolet and Visible Spectrum of Comet 122P/DE VICO to Identify the Parent Molecule CS_2. *Astrophys. J.* **2004**, *607* (2), L139−L141.
(22) Bockelée-Morvan, D.; Crovisier, J.; Mumma, M. J.; Weaver, H. A. The Composition of Cometary Volatiles. *Comets II* **2004**, 391−423.
(23) Jiménez-Escobar, A.; Muñoz Caro, G. M.; Ciaravella, A.; Cecchi-Pestellini, C.; Candia, R.; Micela, G. Soft X-Ray Irradiation of H_2S Ice and the Presence of S_2 in Comets. *Astrophys. J., Lett.* **2012**, *751* (2), L40.
(24) De Sorgo, M.; Yarwood, A. J.; Strausz, O. P.; Gunning, H. E. Photolysis of Carbon Disulfide and Carbon Disulfide-Oxygen Mixtures. *Can. J. Chem.* **1965**, *43* (6), 1886−1891.
(25) Makarov, V. I.; Bazhin, N. M. The Influence of a Magnetic-Field on the Fluorescence and Photolysis Rate of Carbon-Disulfide Vapor. *Chem. Phys. Lett.* **1986**, *124* (6), 499−503.
(26) Makarov, V. I. The Pressure-Dependence of Fluorescence Intensity and Photolysis Rate of the Vapors of Carbon Bisulfide, Nitrogen-Dioxide, and Sulfur-Dioxide. *Int. J. Chem. Kinet.* **1990**, *22* (1), 1−19.
(27) Sapers, S. P.; Donaldson, D. J. Two-Photon Photochemistry of CS_2 - Formation of S_2(V-LESS-THAN-OR-EQUAL-TO-2) and CS(V-LESS-THAN-OR-EQUAL-TO-10) at 308 nm. *J. Phys. Chem.* **1990**, *94* (26), 8918−8921.
(28) Trabelsi, T.; Al-Mogren, M. M.; Hochlaf, M.; Francisco, J. S. Mechanistic Study of the Photoexcitation, Photoconversion, and Photodissociation of CS_2. *J. Chem. Phys.* **2018**, *149* (6), 064304.
(29) Zhou, J. M.; Zhao, Y. R.; Hansen, C. S.; Yang, J. Y.; Chang, Y.; Yu, Y.; Cheng, G. K.; Chen, Z. C.; He, Z. G.; Yu, S. R. Ultraviolet Photolysis of H_2S and Its Implications for SH Radical Production in the Interstellar Medium. *Nat. Commun.* **2020**, *11* (1), 1547.
(30) Chang, Y.; He, Z. G.; Luo, Z. J.; Zhou, J. M.; Zhang, Z. G.; Chen, Z. C.; Yang, J. Y.; Yu, Y.; Li, Q. M.; Che, L.; et al. Application of Laser Dispersion Method in Apparatus Combining H Atom Rydberg Tagging Time-of-Flight Technique with Vacuum Ultraviolet Free Electron Laser (dagger). *Chin. J. Chem. Phys.* **2020**, *33* (2), 139−144.
(31) Chang, Y.; Yang, J. Y.; Chen, Z. C.; Zhang, Z. G.; Yu, Y.; Li, Q. M.; He, Z. G.; Zhang, W. Q.; Wu, G. R.; Ingle, R. A.; et al. Ultraviolet Photochemistry of Ethane: Implications for the Atmospheric Chemistry of the Gas Giants. *Chem. Sci.* **2020**, *11* (19), 5089−5097.
(32) Chang, Y.; Yu, S. R.; Li, Q. M.; Yu, Y.; Wang, H. L.; Su, S.; Chen, Z. C.; Che, L.; Wang, X. G.; Zhang, W. Q. Tunable VUV Photochemistry Using Vacuum Ultraviolet Free Electron Laser Combined with H-atom Rydberg Tagging Time-of-Flight Spectroscopy. *Rev. Sci. Instrum.* **2018**, *89* (6), 063113.
(33) Chang, Y.; Yu, Y.; Wang, H. L.; Hu, X. X.; Li, Q. M.; Yang, J. Y.; Su, S.; He, Z. G.; Chen, Z. C.; Che, L. Hydroxyl Super Rotors from Vacuum Ultraviolet Photodissociation of Water. *Nat. Commun.* **2019**, *10*, 1250.
(34) Wang, H. L.; Yu, Y.; Chang, Y.; Su, S.; Yu, S. R.; Li, Q. M.; Tao, K.; Ding, H. L.; Yang, J. Y.; Wang, G. L. Photodissociation Dynamics of H_2O at 111.5 nm by a Vacuum Ultraviolet Free Electron Laser. *J. Chem. Phys.* **2018**, *148* (12), 124301.
(35) Li, Z. X.; Zhao, M.; Xie, T.; Chang, Y.; Luo, Z. J.; Chen, Z. C.; Wang, X. G.; Yuan, K. J.; Yang, X. M. Velocity Map Imaging Studies of the Photodissociation of CS_2 by Two-Photon Excitation at around 303−315 nm. *Mol. Phys.* **2020**, e1813911.
(36) Fournier, J.; Lalo, C.; Deson, J.; Vermeil, C. Thermoluminescence Following VUV Photolysis of OCS and CS_2 in an Argon Matrix. *J. Chem. Phys.* **1977**, *66* (6), 2656−2659.
(37) Carleer, M.; Colin, R. $f^1\Delta_u$-$a^1\Delta_g$ Band System of S_2 in Absorption. *J. Phys. B: At. Mol. Phys.* **1970**, *3* (12), 1715−1723.
(38) Jungen, C.; Malm, D. N.; Merer, A. J. Analysis of a $^1\Delta_u$-$^1\Sigma^+_g$ Transition of CS_2 in near Ultraviolet. *Can. J. Phys.* **1973**, *51* (14), 1471−1490.
(39) Kasahara, H.; Mikami, N.; Ito, M.; Iwata, S.; Suzuki, I. Excitation and Dispersed Fluorescence-Spectra of the $^1B_2$(V)-$^1\Sigma^+_g$(X) Transition of Jet-Cooled CS_2. *Chem. Phys.* **1984**, *86* (1−2), 173−188.
(40) Kawasaki, M.; Sato, H.; Kikuchi, T.; Fukuroda, A.; Kobayashi, S.; Arikawa, T. Angular-Distributions of Photofragments Generated in the Two-Photon Dissociation of Nitrogen-Dioxide and Carbon-Disulfide. *J. Chem. Phys.* **1987**, *86* (8), 4425−4430.

■ NOTE ADDED AFTER ASAP PUBLICATION

Due to an ACS production error, this paper was originally published ASAP with incorrect pagination. This was corrected in the version published on January 14, 2021.

https://dx.doi.org/10.1021/acs.jpclett.0c03386
J. Phys. Chem. Lett. 2021, 12, 844−849